



Universidad de Valladolid



**ESCUELA DE INGENIERÍAS
INDUSTRIALES**

UNIVERSIDAD DE VALLADOLID

ESCUELA DE INGENIERIAS INDUSTRIALES

Grado en Ingeniería Electrónica Industrial y Automática

**COUPLING OF MECHANICAL AND ELECTRICAL
CONTACT BEHAVIOR OF CURRENT CARRYING
CONNECTIONS IN FINITE ELEMENT MODELS**

Autor:

Santana Riesco, Gonzalo

Responsable de Intercambio en la Uva:

Eusebio de la Fuente

Universidad de destino

Technische Universität Dresden

Valladolid, septiembre de 2021.

TFG REALIZADO EN PROGRAMA DE INTERCAMBIO

TÍTULO: COUPLING OF MECHANICAL AND ELECTRICAL CONTACT BEHAVIOR OF
CURRENT CARRYING CONNECTIONS IN FINITE ELEMENT MODELS

ALUMNO: Gonzalo Santana Riesco

FECHA: 20/09/2021

CENTRO: IEEH (Institute of Electrical Power Systems and High Voltage
Engineering)

UNIVERSIDAD: Technische Universität Dresden

TUTOR: Dr.-Ing. Christian Hildmann

Resumen:

El acoplamiento del comportamiento mecánico y eléctrico de los contactos eléctricos para geometrías y materiales básicos es bien conocido y puede describirse analíticamente. Sin embargo, para las conexiones reales se determina hasta ahora empíricamente. Es sabido que la resistencia eléctrica disminuye al aumentar la fuerza de compresión. En este trabajo, se evalúan los resultados existentes de los ensayos de compresión y las resistencias de conexión medidas para una conexión específica, con sus distintas dimensiones. A partir del análisis de los resultados empíricos, se ha creado un modelo de elementos finitos con el programa Ansys que tiene en cuenta la interacción del comportamiento mecánico y eléctrico del contacto. El modelo se utiliza para calcular la resistencia eléctrica de la unión en función del esfuerzo de compresión aplicado. De esta forma, ya no es necesario realizar experimentos reales de dicho contacto eléctrico ya que la simulación en elementos finitos es suficiente.

Palabras clave:

Elementos finitos, simulación, acoplamiento mecánico-eléctrico, contacto eléctrico, tratamiento de datos.

Abstract:

The coupling of mechanical and electrical behaviour of electrical contacts for basic contact geometries and materials is well known and can be described analytically. However, for real connections it is so far determined empirically. It is known that the electrical contact resistance decreases with increasing compressive strength. In this work, existing results from compression tests and measured connection resistances are evaluated for a specific connection. From the analysis of the empirical results, a finite element model has been created with the Ansys program that takes into account the interaction of the mechanical and electrical behaviour of the contact. The model is used to calculate the electrical resistance of the joint as a function of the applied compressive stress. In this way, it is no longer necessary to carry out real experiments on the electrical contact as the finite element simulation is sufficient.

Keywords:

Finite elements, simulation, mechanical-electrical coupling, electrical contact, data treatment.



Studienarbeit

COUPLING OF MECHANICAL AND ELECTRICAL CONTACT BEHAVIOR OF CURRENT-CARRYING CONNECTIONS IN FINITE ELEMENT MODELS

Santana, Gonzalo
17.02.1999 in Valladolid, Spain

Verantwortliche Hochschullehrer / 1. Gutachter:

PD Dr.-Ing. Stephan Schlegel

Betreuer:

Dr.-Ing. Christian Hildmann

eingereicht am 23.08.2021

Blank page for assignment

(please scan for the digital version)

Declaration of independence

I hereby certify that I have prepared this thesis without the unauthorised assistance of third parties and without the use of resources other than those indicated; the ideas taken directly or indirectly from external sources are identified as such. In the selection and evaluation of the material as well as in the production of the manuscript, I have received support from the following persons:

Dr.-Ing. Christian Hildmann

No other persons were involved in the intellectual production of the present work. I am aware that failure to comply with this declaration may result in the subsequent withdrawal of the diploma degree / master's degree.

Dresden, 23.08.2021

Signature

(Please scan for the digital version)

Abstract

The coupling of mechanical and electrical contact behaviour for basic contact geometries and materials is well known and can be described analytically. The coupling of mechanical and electrical contact behaviour for real current-carrying connections is so far determined empirically from experiments. In this work, existing results from compression tests and measured connection resistances are evaluated for a specific connection. Further, a finite element model has been setup, which considers the interaction of mechanical and electrical contact behaviour. The model is used to calculate the joint resistance depending on the applied compressive stress.

The first task consists of the literature study on the mechanical and electrical behaviour of current-carrying connections, approaches to calculate the real area of contact as well as contact resistance and the capabilities of finite element programs. After that, the next step is the creation of mechanical and electrical finite element models in Ansys of the current-carrying connections with copper busbars, and the coupling of the two models. Finally, analyses depending on the geometry of the busbars will be carried out, to check whether it is possible to adapt the model for different busbars geometries.

To conclude, the coupling of mechanical and electrical contact behaviour has been successfully modelled in a finite element model, where the joint resistance is calculated depending on the applied compressive stress, and a general model for the different busbar geometries has been obtained.

Keywords: coupled model, finite element, mechanical and electrical contact, joint resistance, electrical contact, modelling.

Contents

1	Introduction	1
2	State of knowledge.....	2
2.1	Theory of electrical contacts.....	2
2.1.1	Electrical constriction resistance.....	2
2.1.2	Multiple contact spots	2
2.1.3	Film resistance.....	3
2.2	Empirical description for electrical contacts	3
2.3	Geometrical factors.....	5
2.4	Capabilities of FEM programs	6
2.4.1	Coupling of fields.	7
2.4.2	Rough surface generation procedure	8
3	Specification of the task	11
4	Electrical and mechanical calculations	12
4.1	Geometry	12
4.2	Description of experimental data	12
4.3	Electrical model	13
4.3.1	Setup	13
4.3.2	Procedure	14
4.3.3	Results.....	14
4.4	Mechanical model	17
4.4.1	Setup	17
4.4.2	Results.....	18
4.5	First coupled model	18
5	Coupled calculations	20

5.1	Ecc dependance on stress	20
5.1.1	Correlation between ecc-value and stress.....	20
5.2	Final coupled model.....	22
5.2.1	Setup	22
5.2.2	Procedure	25
5.2.3	Results.....	26
6	Summary and outlook.	29
7	Directories	31
8	Annexes	34
8.1	Usercnprop use	34
8.2	Other geometries results.....	35

Variables, meaning and units

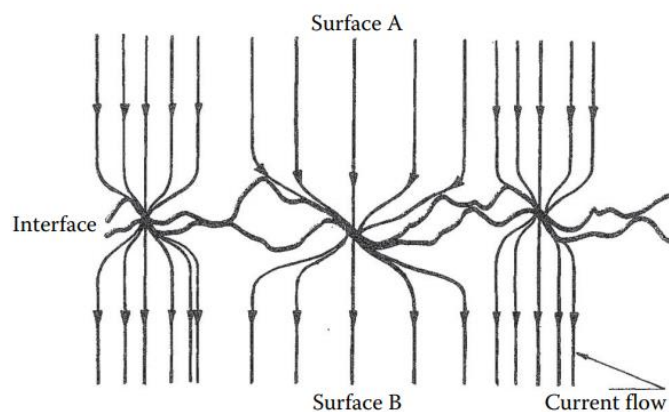
A_c	Area of mechanical contact	m^2
a	Radius of a-spot	m
a, b	Semiaxes of elliptical a-spot	m
e	Describes the streamline effect	
ECC	Electric contact conductance	S/m^2
F	Mechanical force	N
H	Hardness of the material	Pa
I	Electrical current	A
J_H	Joule heat power loss per volume	W/m^3
L, w, t	Length, width and height	m
P_J	Power losses due to Joule effect	W
R_b	Bulk resistance	Ω
R_c	Contact resistance	Ω
R_{cS}	Constriction resistance	Ω
R_F	Film resistance	Ω
R_S	Spreading resistance	Ω
R_v	Joint resistance	Ω
s	Thickness of the film	m
V	Voltage drop	V
α	Radius of the cluster of a-spot	m
ρ	Resistivity	Ωm
σ	Normal Stress	MPa
σ_F	Resistance of the film across one m^2	Ω/m^2

1 Introduction

Bolting and clamping are the most common methods to join copper busbars. They are used in electrical power engineering systems to connect operating equipment and must operate safe and reliable during the lifetime of decades.

Bad electrical contacts or electrical contact failure affect both the performance and safety of the components and systems they serve. Contact failure increases the resistance of the conductor and prevents proper current flow. In critical cases, electrical contact resistance causes overheating, which compromise the safety and security of operators and the facility as a whole.

In a bulk electrical junction, the electric current lines become increasingly distorted as the contact interface is approached and the flow lines bundle together to pass through the separate contact spots. Constriction of the electric current by a-spots reduces the volume of material used for electrical conduction and thus increases electrical resistance [1].



Picture 1: Constriction of the current flow at a contact interface

If a contact force is applied between the two surfaces, the area of true contact increases, and so the electrical resistance of the connection decreases [1]. Using FEM programs to implement this behaviour in models is now a common practice to carry out analysis of the connections. The correlations are explained more in detail in the following sections.

2 State of knowledge

2.1 THEORY OF ELECTRICAL CONTACTS

2.1.1 ELECTRICAL CONSTRICTION RESISTANCE

The simplest analytical evaluation of the constriction resistance generally assumes a-spots to be circular [1].

The spreading resistance in the half space near a circular a-spot is given as [1]

$$R_s = \frac{\rho}{4a} \quad (1)$$

The total constriction resistance for the entire contact is, thus, twice the spreading resistance or [1]

$$R_{cs} = \frac{\rho}{2a} \quad (2)$$

If the upper and lower half of a contact consist respectively of materials with resistivity ρ_1 and ρ_2 , the electrical constriction resistance, then, becomes [1]

$$R_{cs} = \frac{\rho_1 + \rho_2}{4a} \quad (3)$$

2.1.2 MULTIPLE CONTACT SPOTS

In practice, contact between nominally flat surfaces occurs at clusters of a-spots. The positions of the clusters are determined by the large-scale waviness of the contact surfaces, and the a-spots by the small-scale surface roughness [1].

In the simplest case of a large number n of circular a-spots situated within a single cluster, to a good approximation, the contact resistance is given as [1]

$$R_{cs} = \rho \left(\frac{1}{2na} + \frac{1}{2\alpha} \right) \quad (4)$$

where a is the mean a-spot and α is the radius of the cluster [1].

2.1.3 FILM RESISTANCE

If a single a-spot is completely covered with a thin film of the resistivity ρ_F and a thickness s , the film resistance is given by [2]:

$$R_F = \frac{\rho_F s}{\pi a^2} = \frac{\sigma_F}{\pi a^2} \quad (5)$$

with σ_F as tunnel resistivity i.e. the resistance of the film across one m^2 [2].

The total contact resistance (R_c) of a contact between two contacting metallic surfaces consists of the constriction resistance (R_{cs} , eq. (2)) and the resistance of the film (R_F , eq. (5)), that is:

$$R_c = R_{cs} + R_F = \frac{\rho}{2a} + \frac{\sigma_F}{\pi a^2} \quad (6)$$

The joint resistance (R_v) of a joint between two contacting metallic surfaces is the sum of the contact resistance, eq. (6), and the bulk resistance, which is the resistance of the metallic material:

$$R_v = R_c + 2R_b = R_{cs} + R_F + 2R_b = \frac{\rho}{2a} + \frac{\sigma_F}{\pi a^2} + 2R_b \quad (7)$$

2.2 EMPIRICAL DESCRIPTION FOR ELECTRICAL CONTACTS

The details of the number and spatial distribution of the a-spots are not important to the evaluation of contact resistance in many practical applications [1].

It is generally accepted that the true contact area is controlled by the **plastic deformation** of the asperities projecting from the surface. The area of mechanical contact, A_c , is related to the load F applied to the electrical interface and to the plastic flow stress (or hardness) H of the softer material as [1]

$$F = A_c \cdot H \quad (8)$$

Expression (8) is extremely important and relevant for the interpretation of measurements of electrical contact resistance. It states that the area of mechanical contact between two surfaces is independent of the area of nominal contact of the

surfaces. That is, $A_c = \frac{F}{H}$ depends only on the contact force and the hardness of the contacting bodies, and it is independent of the dimensions of the contacting objects. Equation (8) is valid under conditions of plastic deformation [1].

If the electrical interface does not carry electrically insulating films and is characterized by a sufficiently large number of a-spots distributed within a Holm radius α , the data suggest that the contact resistance can be approximated as [1]

$$R_c = \frac{\rho}{2\alpha} \quad (9)$$

The contact resistance may then be expressed as [1]

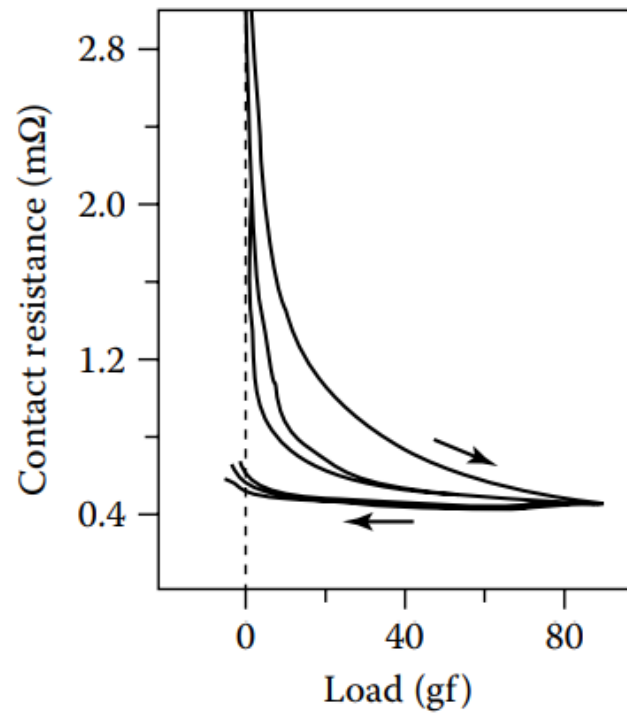
$$R_c = \sqrt{\frac{\rho^2 \eta \pi H}{4F}} \quad (10)$$

This expression is very useful and valid. This estimate generally agrees to 20% or better with actual measured values [1].

The decrease in contact resistance with increasing mechanical load stems from a combination of several factors (Picture 2), the most important ones being [1]:

- An increase in the number of contacting surface asperities as the nominal surfaces are brought closer together under the influence of an increasing load.
- A permanent flattening of the contacting asperities, which reduces the constriction resistance associated with each a-spot, as the area increases first elastically and later plastically, and thus reduces the overall contact resistance.
- Work-hardening of the deformed contact asperities. This last effect decreases the rate at which contacting asperities flatten, and thus, reduces the rate at which new asperities are brought into play as the load is increased further.

Contact resistance increases relatively slowly with decreasing load, after application of the initial load. This stems from permanent flattening and adhesion of the asperities following contact due to the plastic deformation. The little increase of contact resistance when decreasing mechanical load can be explained as there is always some a-spots caused by elastic deformation that disappear [1].



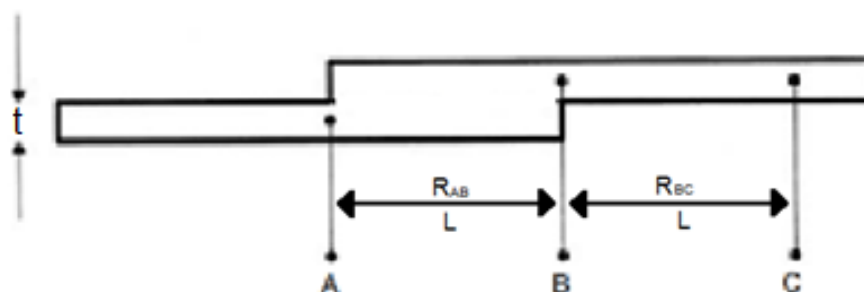
Picture 2: Contact resistance depending on increasing and decreasing load

2.3 GEOMETRICAL FACTORS

The dimensions of the copper busbars are also important for the resistance of the joint as they influence the bulk resistance R_b . A current I , is passed through the busbar from end to end. The voltage drop is measured between A and B, and between B and C. Hence, [3]

$$V_{AB} = R_{AB} \cdot I ; V_{BC} = R_{BC} \cdot I \quad (11)$$

$$e = \frac{V_{AB}}{V_{BC}} = \frac{R_{AB}}{R_{BC}} \quad (12)$$



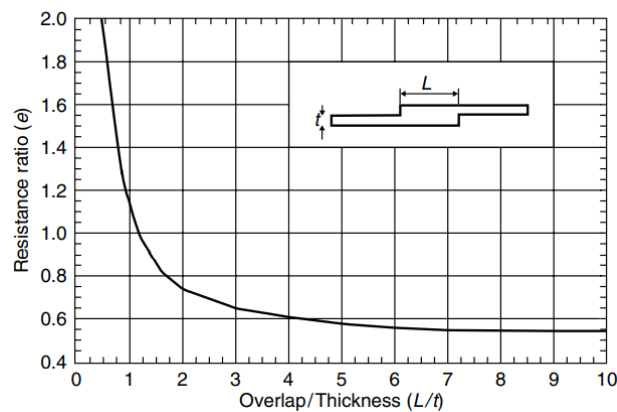
Picture 3: Description of resistance of overlapping busbars

Parameter e describes the streamline effect, R_{AB} is the total resistance of a joint, w is the width of the busbar, t is the height, and R_{BC} is the resistance of equal length of a busbar and is given as [3]

$$R_{BC} = \rho \cdot \frac{L}{wt} \quad (13)$$

Hence, the streamline effect e becomes a function of the ratio L/t , i.e., [3]

$$e = R_{AB} \frac{w}{\rho} \cdot \frac{1}{L/t} \quad (14)$$



Picture 4: Streamline effect graph

The interest is to have the joint resistance as low as possible, this means to have the e -ratio low. Analysing the graph of Picture 4, $\frac{L}{t} = 5$ seems a very optimal overlap/thickness ratio. This is the reason why this ratio is used on the busbars in laboratory tests (see chapter 4.2).

2.4 CAPABILITIES OF FEM PROGRAMS

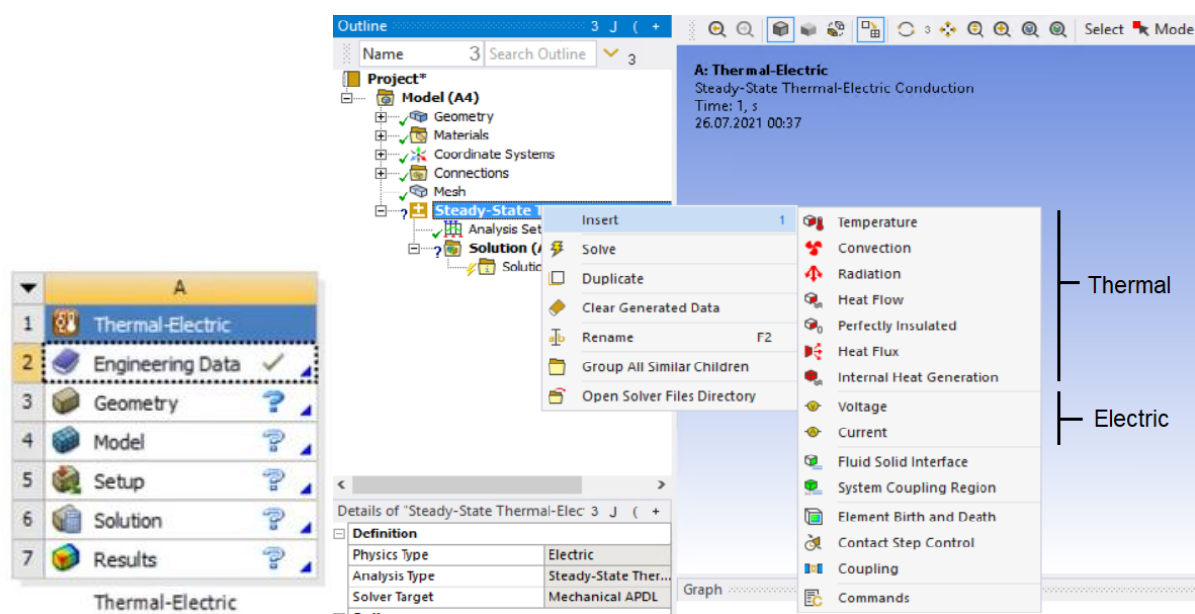
FEM programs are able to do simulations of multi-physics problems, so that the approach to a more realistic study of electrical connections can be done. Therefore, thermal-mechanical-electrical models of contacts have been carried out in several ways. The two main points of the modelling are the coupling of fields, and the contact surface generation.

2.4.1 COUPLING OF FIELDS.

There are different methods for coupling the different physics analysis. The main methods are described below.

2.4.1.1 DIRECT METHOD.

The direct method usually involves only one analysis that uses a coupled-field element type containing all necessary degrees of freedom. It could be the best choice since it can calculate the mechanical, electrical and thermal behaviours simultaneously. However, the computation time is long. This makes using the direct method for the contact modelling unreasonable [4]. On Picture 5 a thermal-electric coupled calculation scheme is shown from Ansys workbench. Both thermal and electrical settings can be set in the same model as initial conditions.

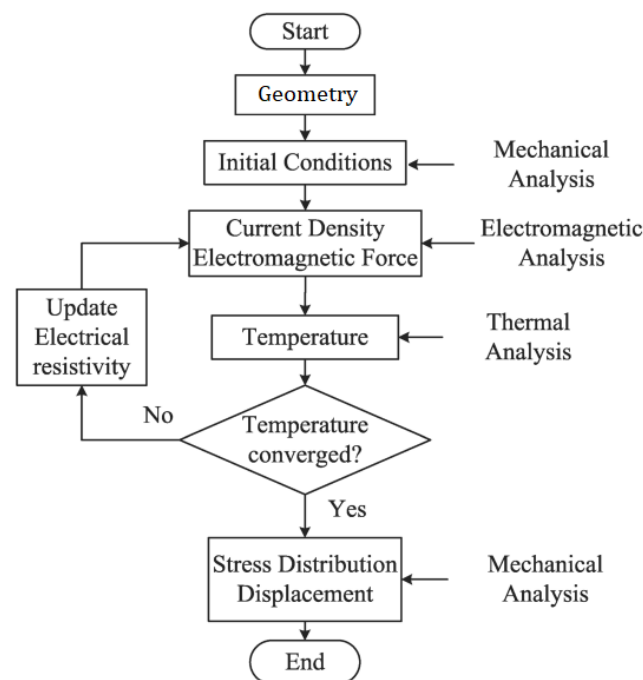


Picture 5. Example of coupling

2.4.1.2 SEQUENTIAL METHOD.

The principle of the sequential method is that the input of one physics analysis depends on the results from another analysis, the analysis are then coupled [4].

In [5] the initial conditions are calculated from mechanical analysis of the plug-in connector. The current density obtained from the electromagnetic analysis is used as an input parameter in the thermal field analysis. The thermal calculation, which uses the electromagnetic force, current density and temperature distribution as load inputs is conducted until the convergence of temperature is achieved. Finally, the mechanical analysis is carried out to find the stress distribution and displacements [5]. This whole explanation is shown in Picture 6.



Picture 6. Flowchart of coupled field calculation process according to [5]

In [7] the routine *usercnprop* can manipulate electrical contact conductance (ECC) and the thermal contact conductance (TCC) values of the contact during the calculation for every time step depending on the contact voltage drop, and the temperatures. This shows a way of changing the parameters of the model. ECC and TCC in this case depend on the results of other analysis (voltage drop and temperatures). This can also be used in the direct coupling method.

2.4.2 ROUGH SURFACE GENERATION PROCEDURE

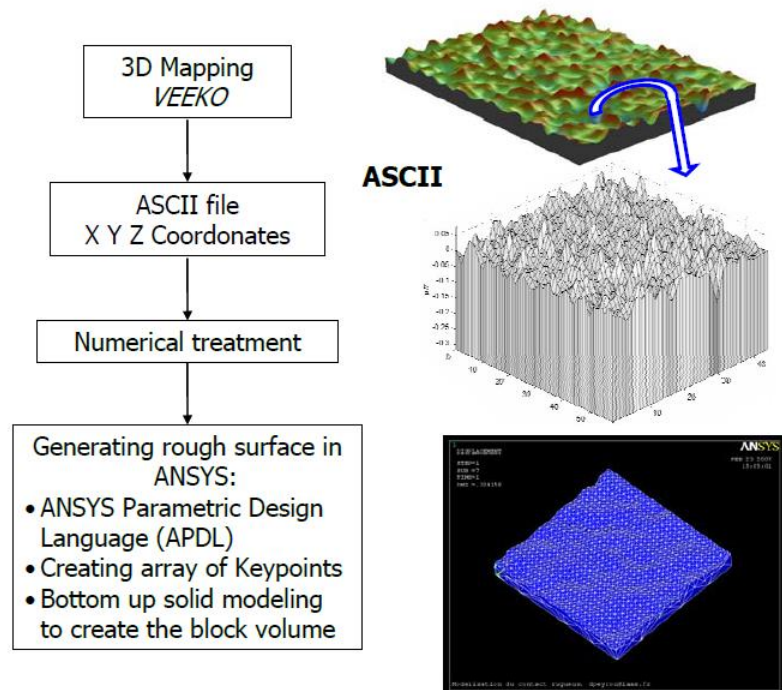
The generation of the contact surface is an important task in a FEA model, as the contact behaviour will depend on the characteristics of the surface generated. There are different

methods for generating the rough contact surface. The main methods are described below.

2.4.2.1 REVERSE ENGINEERING METHOD

Firstly, a 3D mapping of the surface is done using an optical profilometer [6] or atomic force microscopy [4]. Treating the data file using MATLAB and converting it to an ASCII file with XYZ coordinates makes it compatible with ANSYS Parametric Design Language (APDL) [6].

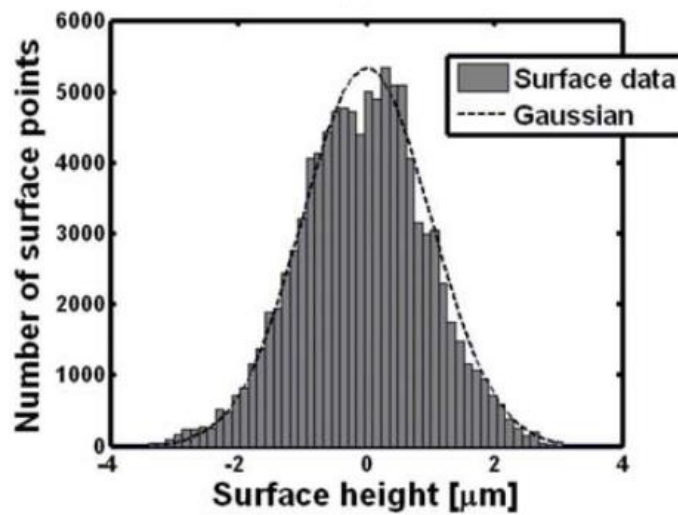
A numerical treatment of the information may be desired, such as the use of some high-pass profile-filter. Thus, only the roughness is recorded and long wave components of the profile trace, e. g. waviness are neglected. [2].



Picture 7: Reverse engineering method

2.4.2.2 APDL FUNCTION

The second method uses the APDL functions such as Gaussian Distribution, $GDIS(x,y)$ where x is the mean and y the standard deviation, to generate a simplified rough surface by creating key points. The mean is null as the macroscopic surface is flat, and the standard deviation is one third of the maximum peak [6].



Picture 8. Height distribution in comparison with an exact Gaussian, from [8].

This method is much simpler and faster than the one explained before in 2.4.2.1. As a consequence, a method, that describes the contact resistance in a multi-spot arrangement depending on the contact force is still not developed

3 Specification of the task

The coupling of mechanical and electrical contact behaviour for basic contact geometries and materials is well known and can be described analytically. The coupling of mechanical and electrical contact behaviour for real current-carrying connections is so far determined empirically from experiments. This behaviour was so far implemented in FEM calculations sequentially using specific simplifications.

In this work, a finite element model in Ansys was setup, which considers the interaction of mechanical and electrical contact behaviour. The approach to the model is different from others, as existing results from compression tests and measured connection resistances are to be evaluated for exemplary busbar connections.

Instead of generating a rough surface, the contact properties are obtained from the experimental data mentioned before, where the given resistance is the joint resistance (equation (7)), considering both the constriction and film effects. As it simulates the assembly of an electrical connection, the model is adapted to consider the increasing load/contact force (Picture 2) results from the laboratory.

The coupling strategy used is the sequential method, mentioned in 2.4.1.2, where the subroutine *usercnprop* manages to change the electrical properties of the contact surface, depending on the stress results obtained before, in the mechanical simulation.

Sensitivity analyses were carried out, depending on the geometry of the busbars, to check whether it is possible to adapt the model for different busbars assemblies.

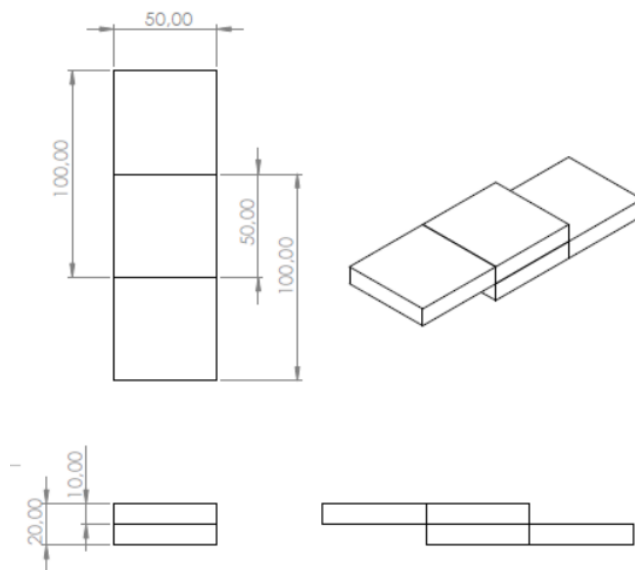
4 Electrical and mechanical calculations

The first thing to start with this work is to setup both the electrical and mechanical models individually of the copper busbars in Ansys. The setup consists of selecting the material used, the geometry of the busbars, what kind of mesh is going to be generated, and the boundary and initial conditions.

4.1 GEOMETRY

Three different busbars geometries depending on the dimensions with the dimensions 25x5x80, 40x8x100 and 50x10x100 (height x base x length in mm).

The geometrical models are done in SolidWorks (Picture 9).



Picture 9: Bodies of the busbars (50x10x100) mm³ for the fem model

4.2 DESCRIPTION OF EXPERIMENTAL DATA

The three busbars' geometries mentioned in 4.1 are the ones used in the laboratory for the tests. For each geometry, there is a set of eight busbars, and the same tests are performed for the four assemblies. The compression tests are performed in a tension-compression testing machine with resistance measurement per force level. The force

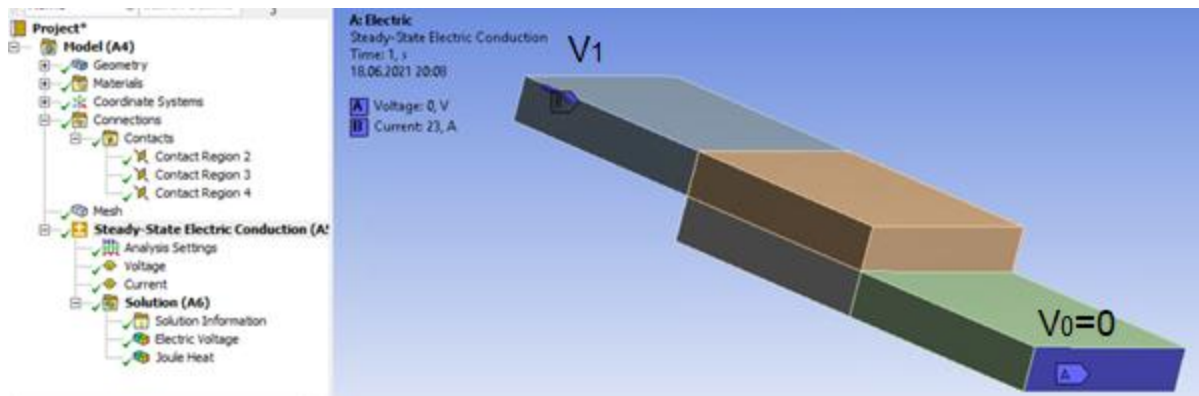
applied goes from 125N to 50 KN and back to 125N in 43 total steps, as loading and unloading of the connection was considered at the laboratory (see Picture 2). The data given provides the joint resistance at the different values of stress for each busbar assembly. Only the loading results from the tests are taken as a reference for the work done in the finite element analysis.

4.3 ELECTRICAL MODEL

4.3.1 SETUP

The material selected for the model is copper alloy, which is already defined in Ansys. The mesh used is generated by the program automatically, as adaptative sizing is enabled, with a resolution of three. The electrical model boundary conditions consist of a 23 A current flowing through the copper busbars, where one end is fixed to a constant voltage of 0 V, see Picture 10. This way, by measuring the other end's voltage V_1 , it is possible to calculate the resistance of the whole busbar assembly, R_T .

$$R_T = \frac{V_1 - V_0}{I} = \frac{V_1}{23 \text{ A}} \quad (15)$$



Picture 10: Boundary conditions

Electric contact conductance, ECC, is used to model current conduction between two contacting surfaces [9], so it is related to the contact resistance. This value is the one that will be varied depending on the load applied when the model is finally coupled. The formula used to obtain the ECC value is:

$$ECC = \frac{1}{R_c \cdot A_c} \quad (16)$$

The ECC-value is obtained from the contact resistance, eq. (16). Taking into consideration the results provided by the laboratory, the contact resistance of the three arrangements was calculated after simulations were carried out. As the given resistance from the experimental data is the joint resistance, eq. (7), the contact resistance needs to be obtained by subtracting the bulk resistance, R_b .

$$R_c = R_v - 2R_b \quad (17)$$

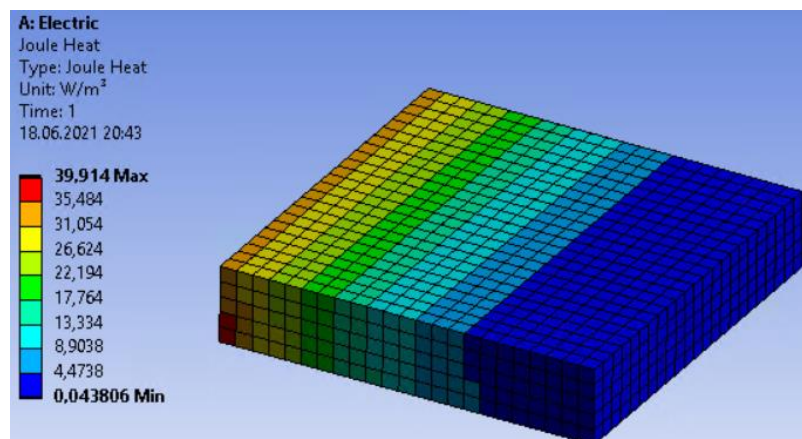
As the bulk resistance for each ECC-Value is not constant, simulations will be carried out to determine its dependence.

4.3.2 PROCEDURE

First, the ECC value will be set manually, and the joint resistance is calculated consequently. The aim is to determine the dependence of joint resistance on ECC, so a relationship between ECC and bulk resistance R_b needs to be found first.

The procedure will consist of running simulations with different values of ECC. The bulk resistance R_b will be calculated from the simulation using the Joule heat solution, see Picture 11. This solution shows the power losses caused by Joule effect, P_j that is described by eq. (18).

$$P_j = I^2 R \quad (18)$$



Picture 11. Joule heat solution in busbar

Hence, current transition in the contact interface of the FEA model does not affect the calculated bulk resistances, and it is possible to obtain it by calculating the total power losses.

4.3.3 RESULTS

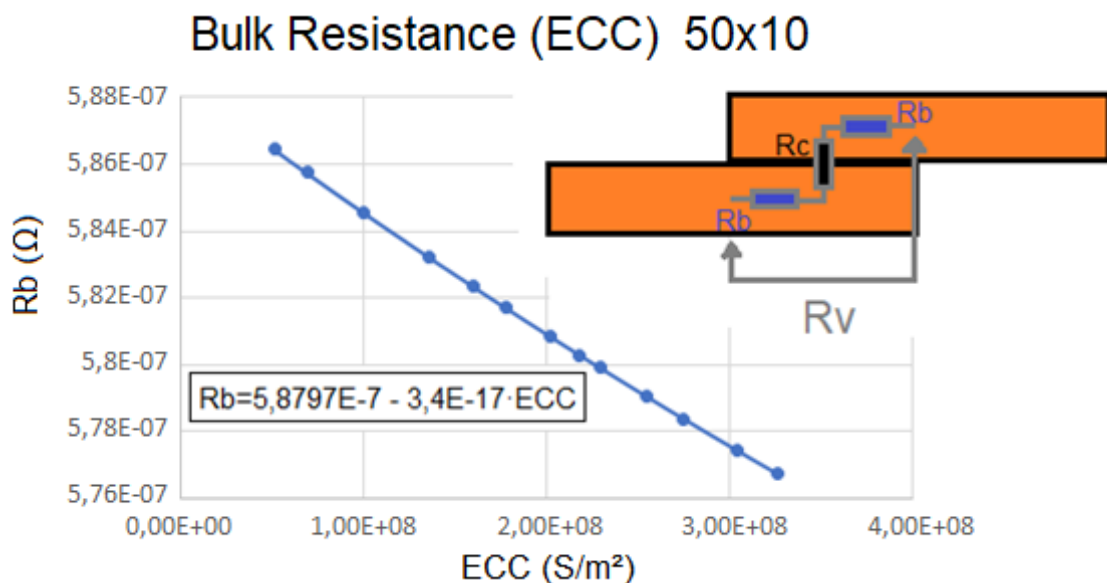
The calculation of the bulk resistance R_b is done with the average Joule heat power loss per volume, J_H ($\frac{W}{m^3}$), that is given by the Ansys solution.

$$P_J = I^2 \cdot R_b = J_H \cdot Vol \Rightarrow R_b = \frac{J_H \cdot Vol}{I^2} = \frac{J_H \cdot 50mm \cdot 50mm \cdot 10mm \cdot 10^{-9}m^3/mm^3}{(23A)^2} \quad (19)$$

In this case the current is set to 23 A, and the volume Vol depends on the geometry of the busbar.

With a parametric study, the calculated values of bulk resistance and its corresponding ECC values can be plotted, where the bulk resistance has a linear dependence on ECC (Picture 12). The bulk resistance decreases very slightly depending on the ECC-value (Picture 12). A linear function can be used to describe the correlation in the considered ECC-range.

$$R_b = 5,8797 \cdot 10^{-7} - 3,4 \cdot 10^{-17} \cdot ECC \quad (20)$$



Picture 12. Bulk resistance dependence on ECC

Now, it is possible to obtain the value of the contact resistance combining equations (16), (17) and (20).

$$R_v = 2R_b + R_c = 2 \cdot (5,8797 \cdot 10^{-7} - 3,4 \cdot 10^{-17} \cdot ECC) + R_c \quad (21)$$

$$R_v = 2 \cdot 5,8797 \cdot 10^{-7} - 2 \cdot \frac{3,4 \cdot 10^{-17}}{R_c \cdot A} + R_c \quad (22)$$

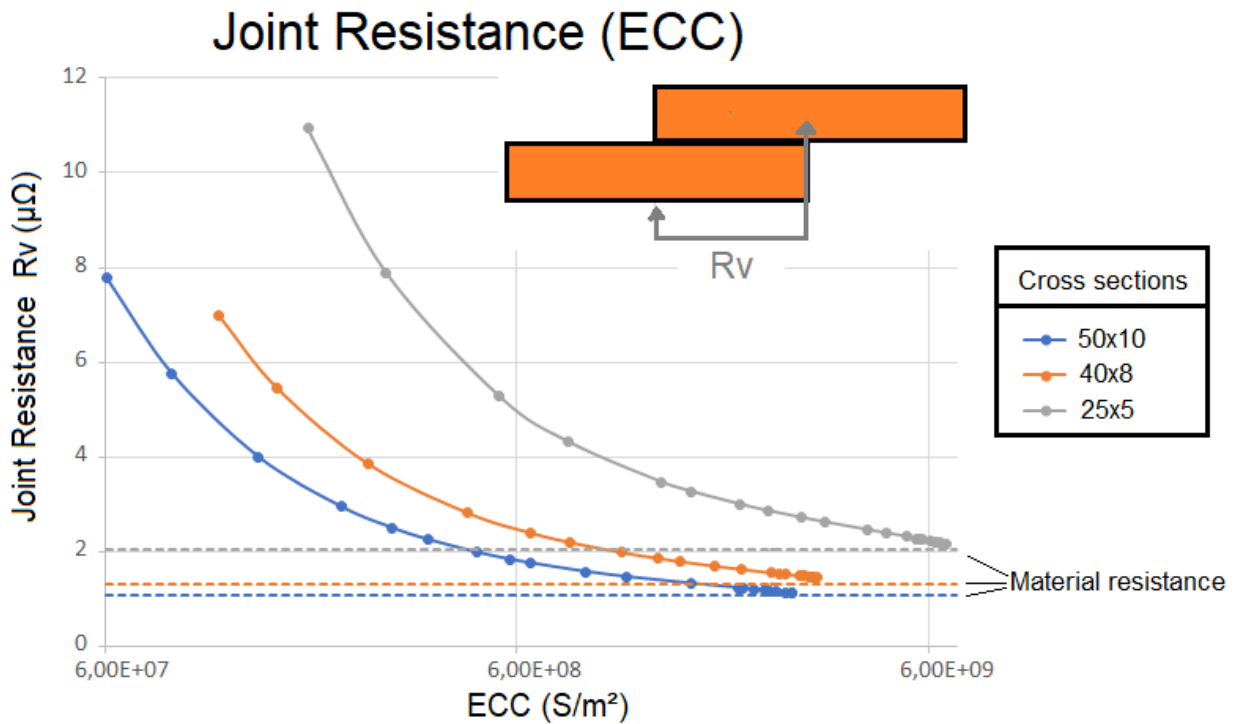
Multiplying the last expression by R_c , the quadratic equation in (23) is obtained.

$$R_c^2 + (2 \cdot 5,8797 \cdot 10^{-7} - R_v) \cdot R_c - \frac{2 \cdot 3,4 \cdot 10^{-17}}{A} = 0 \quad (23)$$

It is now possible to obtain the contact resistance for a known joint resistance, e.g. from experiment, by solving eq. (23).

The linear function that relates ECC to R_b , Picture 12, is different in each busbar arrangement, so it is necessary to run the simulations for the three busbar geometries and then, calculate the contact resistance the same way as mentioned before. Once this is done, obtaining the ECC value for each point is straightforward using equation (16).

Finally, it is possible to show the dependence of joint resistance R_v on electrical contact conductance ECC (Picture 13). As the ECC value grows, the joint resistance gets closer to the value of the material resistance, that is, the bulk resistance. From Picture 13 it can also be noticed that the joint resistance increases as the cross section decreases, which is of course due to material resistance.



Picture 13: Joint resistance depending on ECC-value

4.4 MECHANICAL MODEL

4.4.1 SETUP

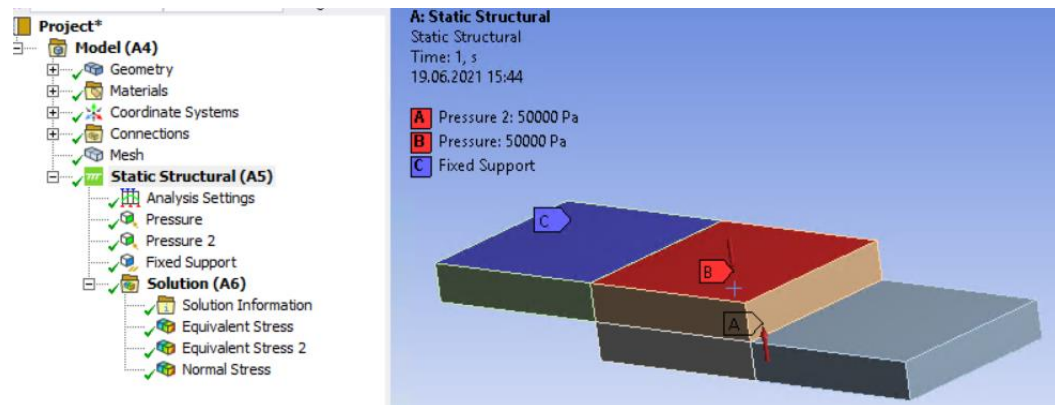
The material selected for the mechanical model is copper alloy, which is already defined in Ansys, see Picture 14. Hence, a purely elastic deformation was considered

Copper Alloy	
Density	8300,0 kg/m ³
Structural	
▼ Isotropic Elasticity	
Derive from	Young's Modulus and Poisson's Ratio
Young's Modulus	1,1e+11 Pa
Poisson's Ratio	0,34000

Picture 14. Structural properties of copper alloy

The mesh used is generated by the program automatically, as adaptive sizing is enabled, with a resolution of three. For the mechanical model the static structural solver will be

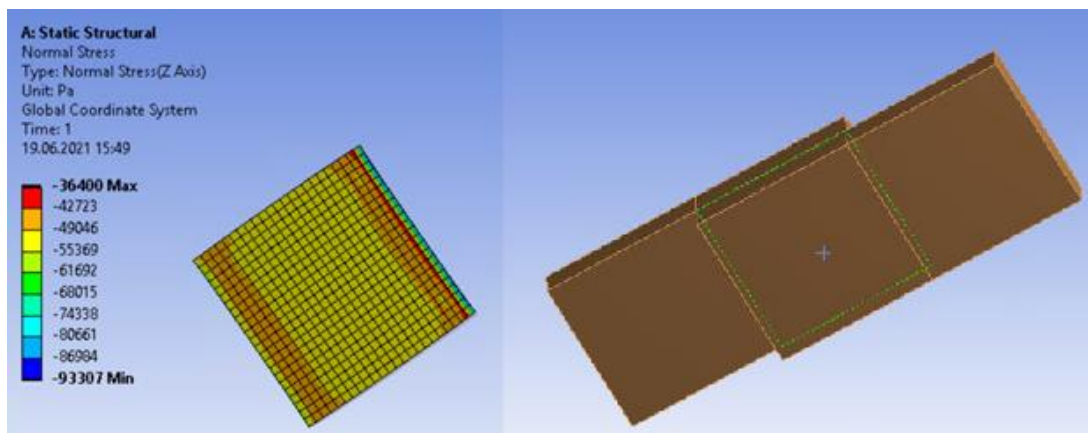
used. The boundary conditions are two equal pressures on the contact faces between the busbars, and a fixed support so the simulation can be solved.



Picture 15: Boundary conditions of mechanical model

4.4.2 RESULTS

The aim of this simulation is to obtain the distribution of normal stress on the contact surface, as it is shown on Picture 16.



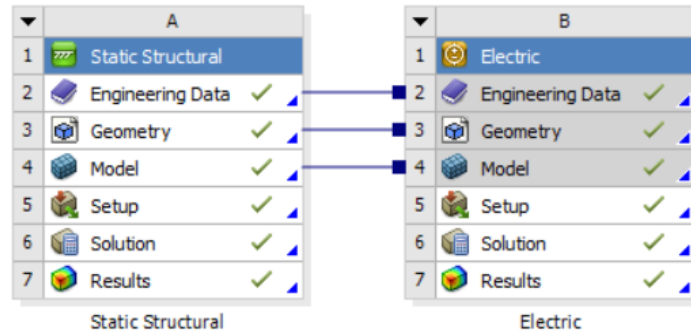
Picture 16: Normal stress distribution in contact surface

In the future coupled model, the normal average stress will be used to calculate the correspondent ECC value, which is of similar value to the applied pressure. For this purpose, the parameterization of this model created here is kept.

4.5 FIRST COUPLED MODEL

The first step for the coupled model is to combine both electric and structural models in the Ansys workbench, enabling data transfer between them (Picture 17). Once this is

done, both simulations can be carried out separately in the same Ansys Mechanical interface. However, those models are not yet coupled. This will be explained in the following sections.



Picture 17: Ansys Workbench

5 Coupled calculations

In this part of the work, the coupled model is set up. First, it is needed to find a function that relates ECC to normal stress at the contact surface. Then, the APDL commands and UPF subroutine must be programmed correctly to implement the coupled behaviour using the function obtained. Finally, a validation of the model is carried out to check the results.

5.1 ECC DEPENDANCE ON STRESS

In order to achieve the coupling of the mechanical and electrical models, it is necessary to know the relationship between ECC and normal stress on the contact surface. The relationships between ECC and contact resistance (equation (16)) and the relationship between contact resistance and stress (equation (10)) are already known. From those equations it is possible to obtain the following function for ECC and the normal stress σ :

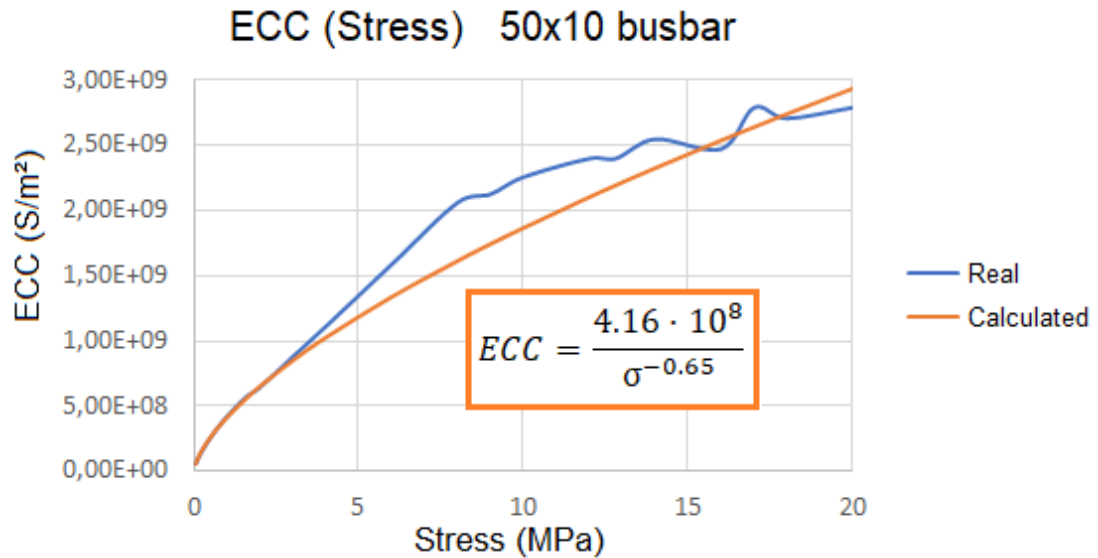
$$ECC = \frac{a}{\sigma^b} \quad (24)$$

Where a and b are parameters that are specific for the contact material as well as for the geometry of the contacts.

5.1.1 CORRELATION BETWEEN ECC-VALUE AND STRESS

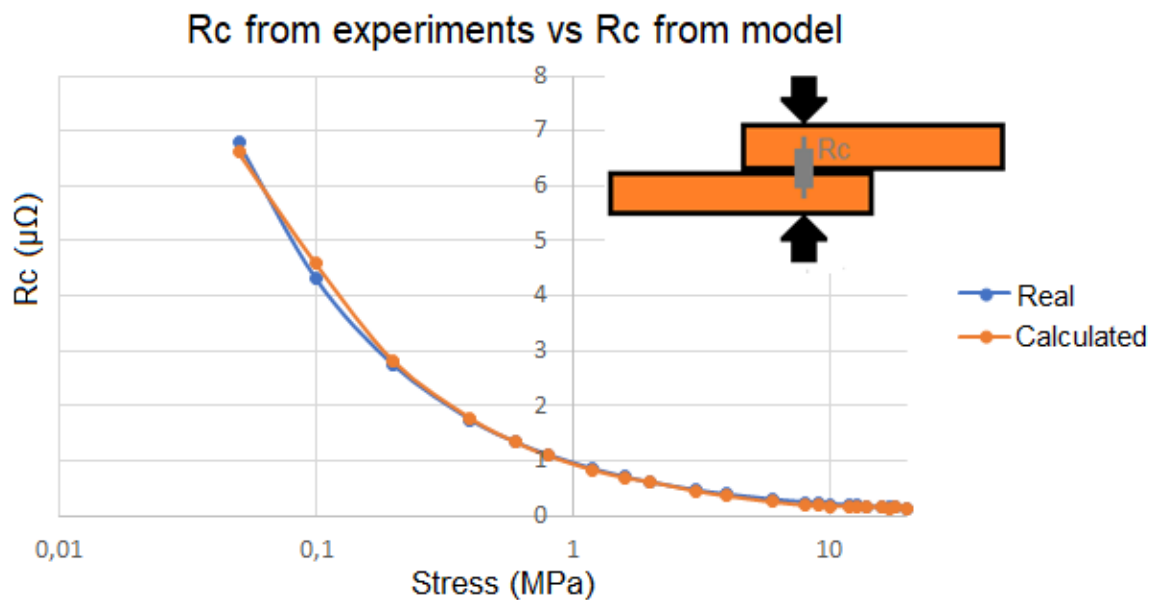
As the value of interest is the contact resistance, the fit will be oriented to minimise the error of the contact resistance obtained from the ECC function, instead of directly minimising the ECC difference from the experimental ECC.

As the ECC values are different for the three geometries, this procedure is repeated accordingly. In the annexes, 8.2, the graphs and fitted curves can be found for the other geometries.



Picture 18. ECC (Stress) fitted curve for 50x10 busbar

Now, in Picture 18 it can be noticed that the ECC fitted curve is not very close to the real values. However, after doing the comparison of the contact resistances obtained using this fit and the experimental ones, in Picture 19, it is obvious to state that this model is precise.



Picture 19. Rc from experiments and model comparison

Therefore, this will be the function relating ECC to stress that will be used in the following coupled calculations. Table 1 shows the parameters a and b of the curve obtained for each geometry.

50x10		40x8		25x5	
a	4,16E+08	a	5,86E+08	a	5,96E+08
b	-0,652	b	-0,657	b	-0,728

Table 1. Parameters of fitted curves

5.2 FINAL COUPLED MODEL

5.2.1 SETUP

In Ansys workbench the setup is the same than in Picture 17 repeated three times, as there are three different busbar geometries, and the boundary conditions of the electrical and mechanical models are the same than described in Picture 10 in 4.3.1, and Picture 15 in 4.4.1, respectively.

5.2.1.1 APDL COMMANDS

Now, it is needed to find a way to hand over the normal stress distribution in the contact surface from the mechanical model to the electrical model. To do so, many ways have been tried with one of them working correctly.

The method that really worked is creating a csv file with the stress components of the contact surface, and then read that file from the electric model. To print the stress components into the file, the PRNSOL command is used.

To create the csv file with the stress data, the next APDL commands are applied in the solution part of the static structural analysis:


```

FILE,file,rst                ! Results are found on 'file.rst'
set,1
! Obtain results on midside nodes
/GRAPHICS,POWER
/EFACET,2                    ! Use 2 facets per edge

! format output for nodes, elements and stress listings
/PAGE, 1E9,, 1E9,,         ! Disable headers
/FORMAT, , ,14,5, ,       ! Fix floating point format
/HEADER, off, off, off, on, off ! Disable summaries
/OUTPUT,STRCAT(jobname,'_result'),csv ! Switch output to file 'JOBNAME.csv'

cmsel,s,K1                  ! Select the contact surface between the busbars
PRNSOL,S,comp              ! Print the stresses components

/OUTPUT                    ! Redirect text output to the file

```

Picture 20. APDL commands in mechanic model

The next step is reading the file from the electrical model in the pre-processor and calculate the average of the stress component that really interests. This is the Z-component as it is the normal stress on the contact surface. Storing that value into an APDL variable makes it possible to be read from the subroutine *usercnprop*. To check that the averaging is well done the result is written into a text file.

Afterwards, the variables containing the parameters a and b of the curves obtained for each geometry are defined, and lastly, the subroutine *usercnprop* is called by the RMODIF command.

The APDL commands for the electric model are shown in Picture 21.

```

cmsel,s,K1                  ! Select contact surface between busbars
*get,node_number,node,0,count ! Counts the nodes of the selected set
*DIM,STRESS_ARRAY,TABLE,node_number-1,6 ! Define array that stores stress data
ALLSEL                    ! Select all nodes again
! Read stress data from the csv file
*TREAD,STRESS_ARRAY,H:\Ansysmodels\50x10\coupled2_files\dp0\SYS\MECH\JOBNAME,csv,,5
*vscfun,AVG_STRESS_APDL,mean,STRESS_ARRAY(0,3) ! Calculate the average of the Z stress component
AVG_STRESS_APDL=-AVG_STRESS_APDL ! Reverse the sign

*cfopen, node_stress_file.txt ! Create a txt file called "node_stress_file.txt"
*vwrite,AVG_STRESS_APDL,node_number ! Write out these values to check it is OK
(4F16.3) ! Define the format
*CFCLOSE ! Close the txt file

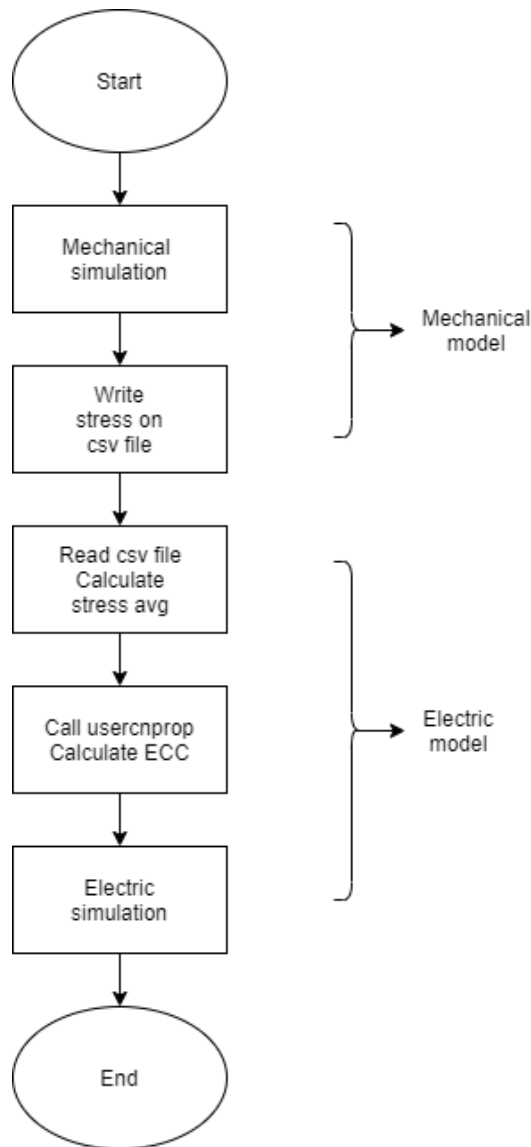
/PREP7                    ! Enter preprocessor
PAR_A_APDL = arg1 ! Parameter A1 of the curve1
PAR_B_APDL = arg2 ! Parameter B1 of the curve1
RMODIF,cid_K1,19,%_CNPROP% ! Redefine ECC value for contact surface
/SOLU                    ! Enter solution processor

```

Picture 21. APDL script in the electrical model

As it was mentioned before, this coupling method is the sequential one, where the output of the mechanical simulation, the stress distribution, is used as an input for the electrical

simulation. To have a better understanding, a flow chart diagram, Picture 22, shows the order of in which the steps are executed during the simulation of the whole coupled model.



Picture 22. Flow chart diagram of the sequential coupling method

5.2.1.2 PROGRAMMING OF UPF SUBROUTINE USERCNPROP

A basic description of what an UPF is and how the usercnprop subroutine is used can be seen in the annexes, 8.1.

Starting from the original *usercnprop.f* script, the variables that are going to be used in the subroutine have to be defined. After that, the data from the APDL variables has to be used in the FORTRAN script, to do so this piece of code has to be implemented, using the *parevl* function:

```
pNameANS = 'AVG_STRESS_APDL'
subc(1)=0.0d0
call parevl(pNameANS,0,subc,2,AVG_STRESS_F,dstr,kerr)
```

Now, the APDL variable AVG_STRESS_APDL is stored into the double precision FORTRAN variable AVG_STRESS_F. This process must be repeated with PAR_A_APDL and PAR_B_APDL in the same way.

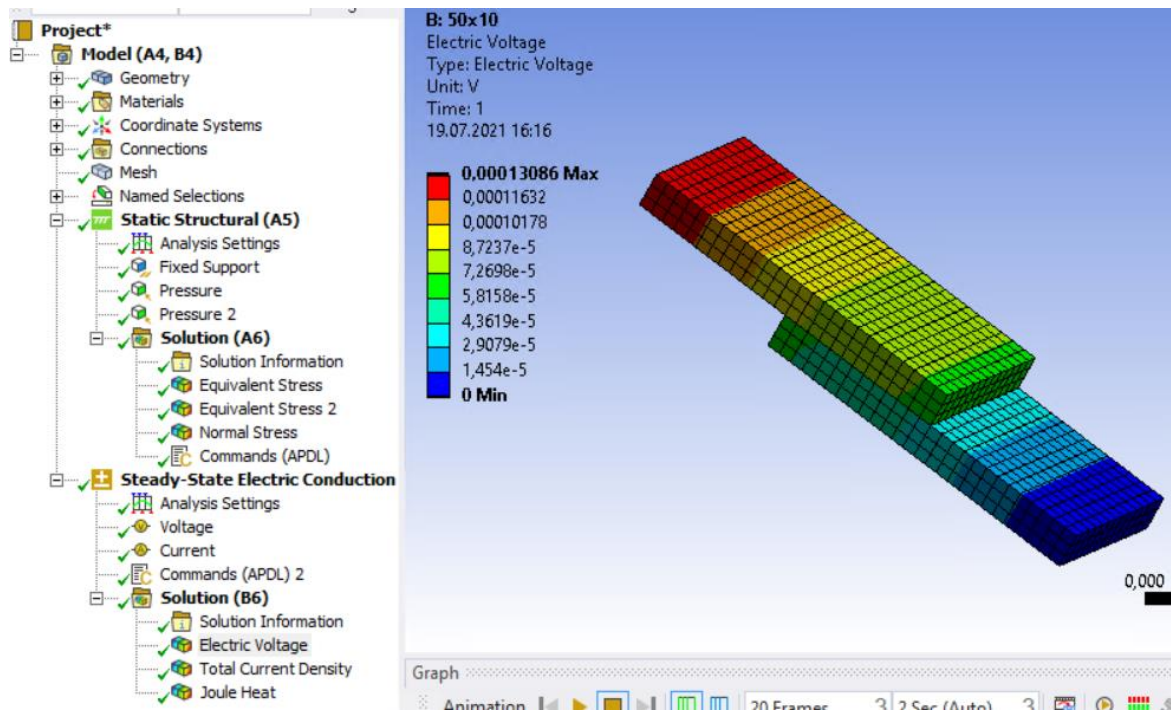
The next step is the implementation of the calculation for ECC in function of the normal stress average in the contact surface (eq. (24)), which is straightforward, as it can be seen on the following code.

```
ECC=PAR_A_F/(0.000001*AVG_STRESS_F)**PAR_B_F
if (kcnprop.eq.19) then
  cnprop(1)=ECC
endif
```

Finally the ECC value is allocated to the real constant *cnprop(1)*. This way, the same script can be used for the different busbar geometries, as the parameters a and b of the curve are treated as inputs.

5.2.2 PROCEDURE

The procedure is very simple. The only input for the mechanical model are the pressures over the busbars. After this is done, the mechanical simulation will be carried out first, and then the electrical simulation automatically according to the flowchart in Picture 22. In the following calculations, the determined dependence of ECC-Value from stress according to chapter 5.1.1 is implemented. One solution from this model is the voltage distribution in the busbars (Picture 23). The maximum voltage in one end is the data needed to calculate the total resistance and the joint resistance of the busbar.



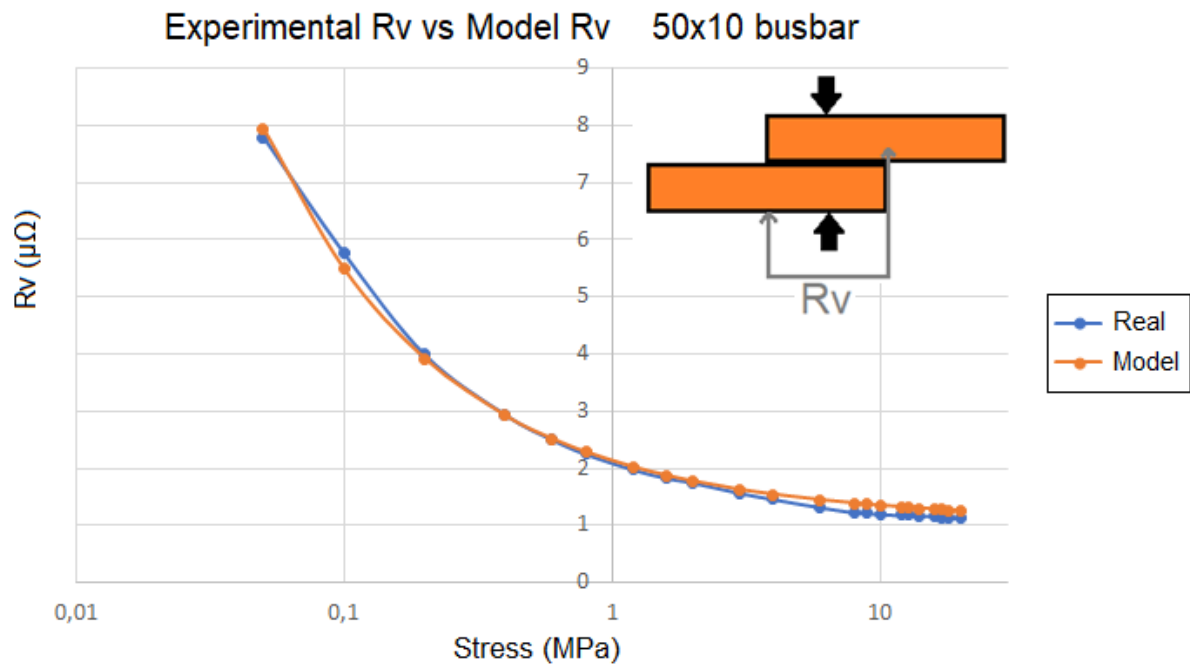
Picture 23. Ansys mechanical interface

5.2.3 RESULTS

To validate the model, the joint resistance must be calculated and compared with the joint resistance obtained in the laboratory tests. To obtain the joint resistance from the model, the procedure is to subtract the material resistance of the non-overlapping busbars from the whole busbar assembly resistance, eq. (15). For the 50x10 busbar the resistances depending on the applied stress can be compared in Table 2 and Picture 24.

50x10 busbar		
Stress (MPa)	Rv (real) $\mu\Omega$	Rv (Model) $\mu\Omega$
0,05	7,79	7,94
0,1	5,76	5,48
0,2	3,99	3,91
0,4	2,94	2,92
0,6	2,5	2,51
0,8	2,25	2,28
1,2	1,98	2,02
1,6	1,83	1,87
2	1,75	1,77
3	1,57	1,62
4	1,46	1,54
6	1,32	1,44
8	1,23	1,38
9	1,22	1,36
10	1,2	1,35
12	1,18	1,32
12,8	1,18	1,31
14	1,16	1,30
16	1,17	1,28
17	1,13	1,27
18	1,14	1,26
20	1,13	1,25

Table 2. 50x10 Rv comparison



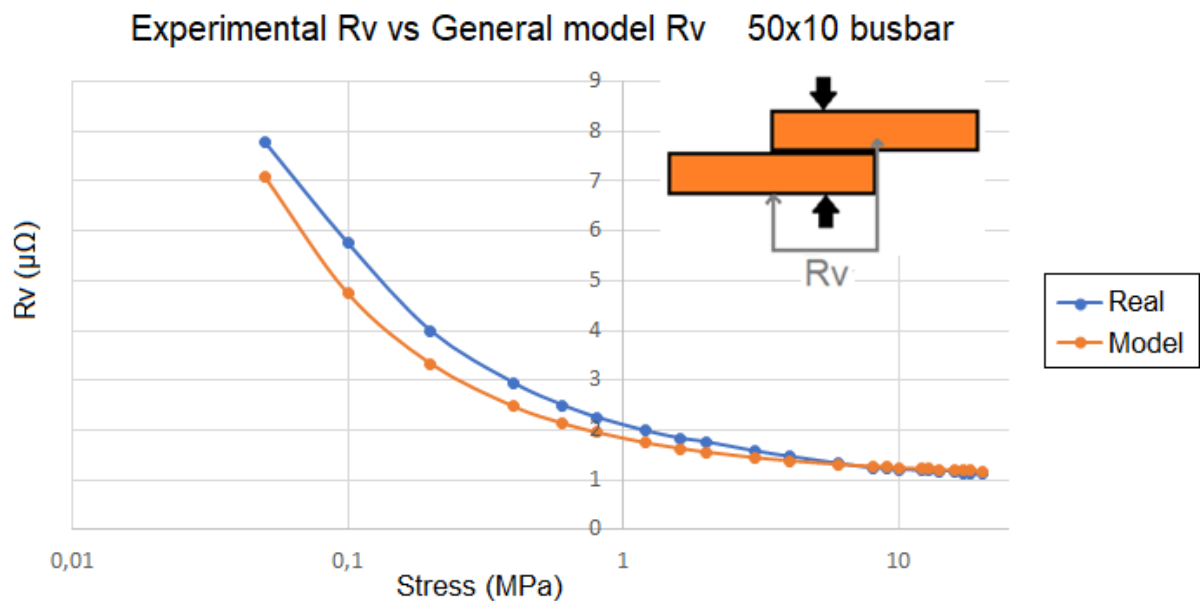
Picture 24. Real vs model joint resistance, 50x10 busbar

The values of joint resistance calculated by the model are very close to the real ones obtained experimentally.

The average relative error along the tested points is 6,75%, 5,28% and 5,02% for the 50x10, 40x8 and 25x5 geometries respectively. These results are satisfactory and prove that the functions of ECC dependence on normal stress are well fitted to the experimental data. This validates the correct modelling carried out.

In the annexes the same results for the other busbar geometries can be found (see 8.2).

ECC's dependence on average normal stress changes for the different busbar geometries. However, using the function obtained for the 25x5 busbar (see Table 1) generates very good results for the other geometries, as the average relative error is 7,6% and 5,5% for the 50x10 (see Picture 25) and 40x8 (see 8.2) busbars respectively. Consequently, this function can be applied for the three geometries as a general model.



Picture 25. Real vs general model joint resistance, 50x10 busbar

6 Summary and outlook.

In this work, a finite element model in Ansys has been setup, which considers the interaction of mechanical and electrical contact behaviour. The approach of the model is different from others, as existing results from compression tests and measured contact resistances have been evaluated for busbars connections.

The electrical contact property, which is the electrical contact conductance value (ECC), is first obtained from the experimental data, where the given resistance is the joint resistance, eq. (7). Then, a fitting analysis is carried out to find a mathematical function of ECC depending on the stress, regarding the minimum error for the contact resistance.

The next step is to implement the model in Ansys. The coupling strategy used is the sequential method, mentioned in 2.4.1.2. The subroutine *usercnprop* manages to change the ECC value of the contact surface, depending on the stress results obtained before, in the mechanical simulation. The way of sending the stress data from the mechanical simulation is by writing a csv file, and then reading it from the electrical simulation. The calculation for the ECC depending on the average stress is determined by the fitted function obtained before from the experimental data.

ECC's dependence on average normal stress is does not differ significantly for the individual busbar geometries. This means that it is possible to find one only function for the different busbar assemblies. If a better fit for the ECC-Stress correlation is found, it can be implemented easily, as it would be just necessary to change the input arguments of parameters a and b in the mechanical Ansys interface.

Once the model has been setup, the way to verify its validity is by comparing the data generated by the model with the empirical data, which in this case is the joint resistance. The model generates solutions very close to the empirical data. This is because it is based on these measures.

A general model capable of predicting the ECC-stress relationship for the different copper busbar geometries has been achieved. The way to validate it as a general model would be

by comparing the simulation results with the results obtained in the laboratory, for a different geometry busbar assembly, e.g., 60x12.

The next step of obtaining a more general contact model is extending its validity for different overlap/thickness ratios (see 2.3), as the busbars tested had all an equal ratio of five.

The most ideal model would be one capable of generating an ECC value for each stress value of a node. In this way, the stress distribution in the contact interface would be considered and such a model could be used for situations where the pressure is not uniform.

7 Directories

Literature

- [1] Slade, P. G.: *Electrical Contacts - Principles and Applications*. 2. Auflage, CRC Press Taylor & Francis Group 2014. - ISBN 978-1-4398-8130-9
- [2] Schoft, Stephan. (2004). Joint resistance depending on joint force of high current aluminum joints. 502 - 510. 10.1109/HOLM.2004.1353163.
- [3] Braunovic, M.: *Electrical Contacts-Fundamentals, Applications and Technology*. Taylor & Francis Group 2006. - ISBN 1-57444-727-0.
- [4] Hong Liu, Dimitri Leray, Patrick Pons, Stéphane Colin. Finite Element Multi-physics Modeling for Ohmic Contact of Microswitches. International Conference on Thermal, Mechanical and Multi-Physics Simulation and Experiments in Microelectronics and Microsystems (EuroSimE), Apr 2014, Ghent, Belgium. pp.Proceedings EuroSimE. (hal-01024132)
- [5] Guan, Xiangyu & Shu, Naiqiu & Kang, Bing & Zou, Minghan. (2015). Multiphysics Analysis of Plug-In Connector Under Steady and Short Circuit Conditions. *Components, Packaging and Manufacturing Technology*, IEEE Transactions on. 5. 320-327. 10.1109/TCPMT.2015.2396197.
- [6] David Peyrou, Fabienne Pennec, Hikmat Achkar, Patrick Pons, Robert Plana. Effect of Contact Force Between Rough Surfaces on Real Contact Area and Electrical Contact Resistance. MEMSWAVE Workshop 2007, Jun 2007, Barcelone, Spain. pp.4. fhal-00172960
- [7] T. Israel, S. Schlegel, S. Großmann, T. Kufner and G. Freudiger, "Modelling of Transient Heating and Softening Behaviour of Contact Points During Current Pulses and Short Circuits," 2019 IEEE Holm Conference on Electrical Contacts, 2019, pp. 9-18, doi: 10.1109/HOLM.2019.8923941.
- [8] Bergstrom, David & Powell, John & Kaplan, A.. (2007). A ray-tracing analysis of the absorption of light by smooth and rough metal surfaces. *Journal of Applied Physics*. 101. 113504-113504. 10.1063/1.2738417.
- [9] Ansys Help 18.2

Pictures

Picture 1: Constriction of the current flow at a contact interface	1
Picture 2: Contact resistance depending on increasing and decreasing load	5
Picture 3: Description of resistance of overlapping busbars.....	5
Picture 4: Streamline effect graph	6
Picture 5. Example of coupling.....	7
Picture 6. Flowchart of coupled field calculation process according to [5].....	8
Picture 7: Reverse engineering method	9
Picture 8. Height distribution in comparison with an exact Gaussian, from [8].	10
Picture 9: Bodies of the busbars (50x10x100) mm ³ for the fem model	12
Picture 10: Boundary conditions.....	13
Picture 11. Joule heat solution in busbar	14
Picture 12. Bulk resistance dependence on ECC	15
Picture 13: Joint resistance depending on ECC-value.....	17
Picture 14. Structural properties of copper alloy	17
Picture 15: Boundary conditions of mechanical model	18
Picture 16: Normal stress distribution in contact surface	18
Picture 17: Ansys Workbench.....	19
Picture 18. ECC (Stress) fitted curve for 50x10 busbar	21
Picture 19. Rc from experiments and model comparison.....	21
Picture 20. APDL commands in mechanic model.....	23
Picture 21. APDL script in the electrical model.....	23
Picture 22. Flow chart diagram of the sequential coupling method.....	24
Picture 23. Ansys mechanical interface.....	26
Picture 24. Real vs model joint resistance, 50x10 busbar	27
Picture 25. Real vs general model joint resistance, 50x10 busbar.....	28
Picture 26. ECC (Stress) fitted curve for 40x8 busbar.....	35
Picture 27. Joint resistance comparison. 40x8 busbar	36
Picture 28. Real vs general model joint resistance, 40x8 busbar	36
Picture 29. ECC (Stress) fitted curve for 25x5 busbar.....	37

Picture 30. Rv comparison. 25x5 busbar.....	38
---	----

Tables

Table 1. Parameters of fitted curves.....	22
Table 2. 50x10 Rv comparison	27
Table 3. 40x8 Rv comparison	35
Table 4. 25x5 Rv comparison	37

8 Annexes

8.1 USERCNPROP USE

The UPF (User Programmable feature) subroutine *usercnprop* is a FORTRAN script that can be programmed to define customized contact properties via real constants, and can be varied due to pressure, penetration, temperature, and your own state variables [9].

The example I am going to do with the subroutine for a first approach consists of changing the ECC value of the contact surface. To call the FORTRAN script some APDL commands may be executed:

```
/PREP7
RMODIF, cid_K1, 19, %_CNPROP%
/SOLU
```

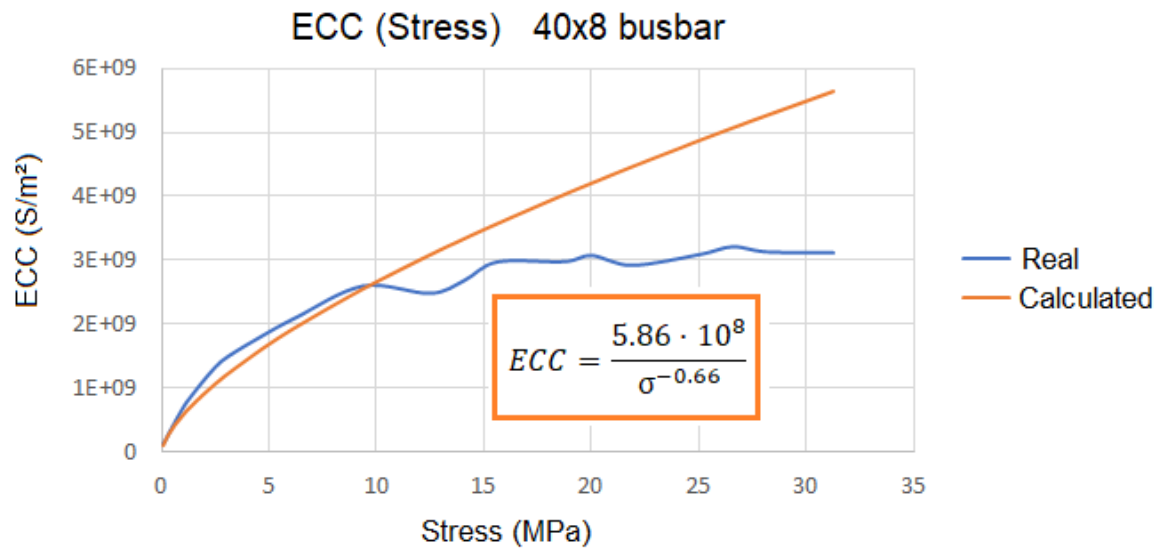
The RMODIF command has 3 arguments; cid_K1 is the id of the contact surface set, 19 is related with the ECC value, and %_CNPROP% calls the *usercnprop.f* script.

In the *usercnprop.f* I just need to add this piece of code:

```
ECC=3.0d8
if (kcnprop.eq.19) then
    cnprop(1) = ECC
endif
```

The way I am compiling the UPF subroutine is by creating a DLL (Dynamic-link library). To build this DLL the FORTRAN script is compiled using ANSUSERSHARED.bat. To avoid problems with the subroutine, the variable ANS_USER_PATH must be related to the path of the directory where the *usercnprop.f* file is located.

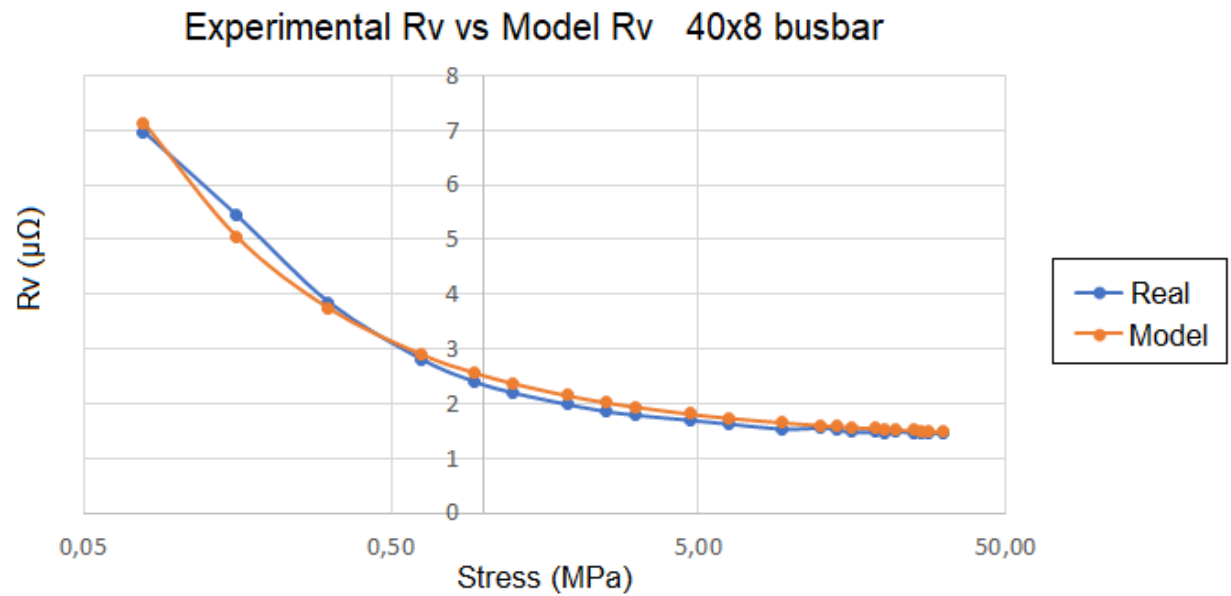
8.2 OTHER GEOMETRIES RESULTS



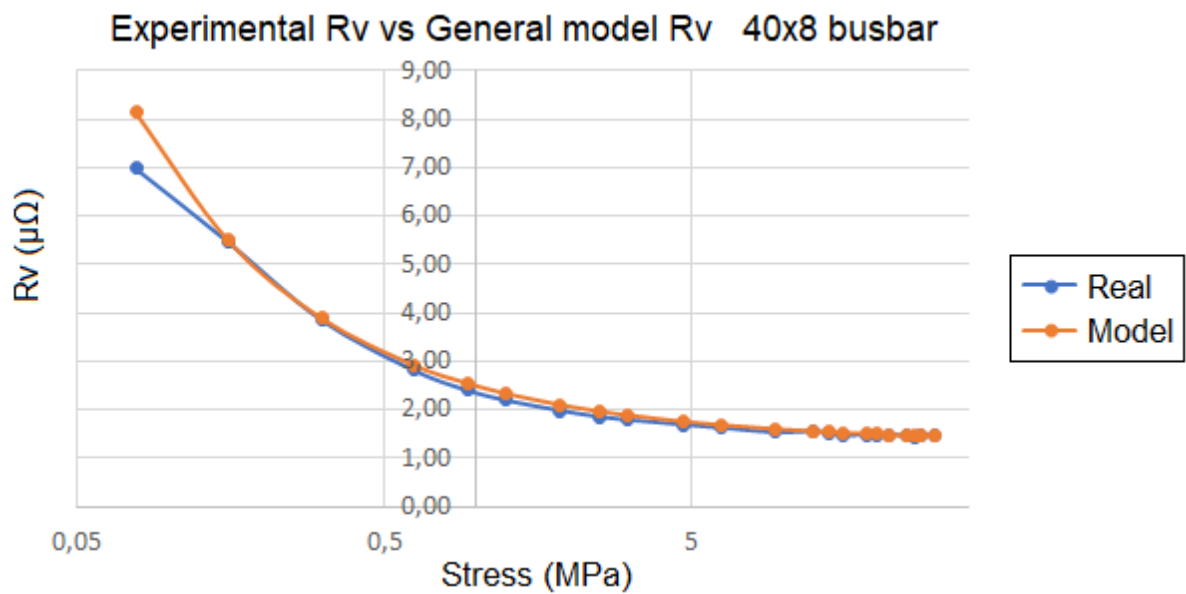
Picture 26. ECC (Stress) fitted curve for 40x8 busbar

40x8 busbar		
Stress (MPa)	Rv (real) $\mu\Omega$	Rv (Model) $\mu\Omega$
0,078125	6,97	7,14
0,15625	5,46	5,06
0,3125	3,86	3,75
0,625	2,82	2,91
0,9375	2,40	2,57
1,25	2,20	2,37
1,875	1,98	2,15
2,5	1,86	2,03
3,125	1,79	1,94
4,6875	1,70	1,82
6,25	1,63	1,74
9,375	1,54	1,66
12,5	1,56	1,61
14,0625	1,52	1,59
15,625	1,48	1,57
18,75	1,48	1,55
20	1,47	1,54
21,875	1,49	1,53
25	1,46	1,51
26,5625	1,45	1,51
28,125	1,46	1,50
31,25	1,46	1,49

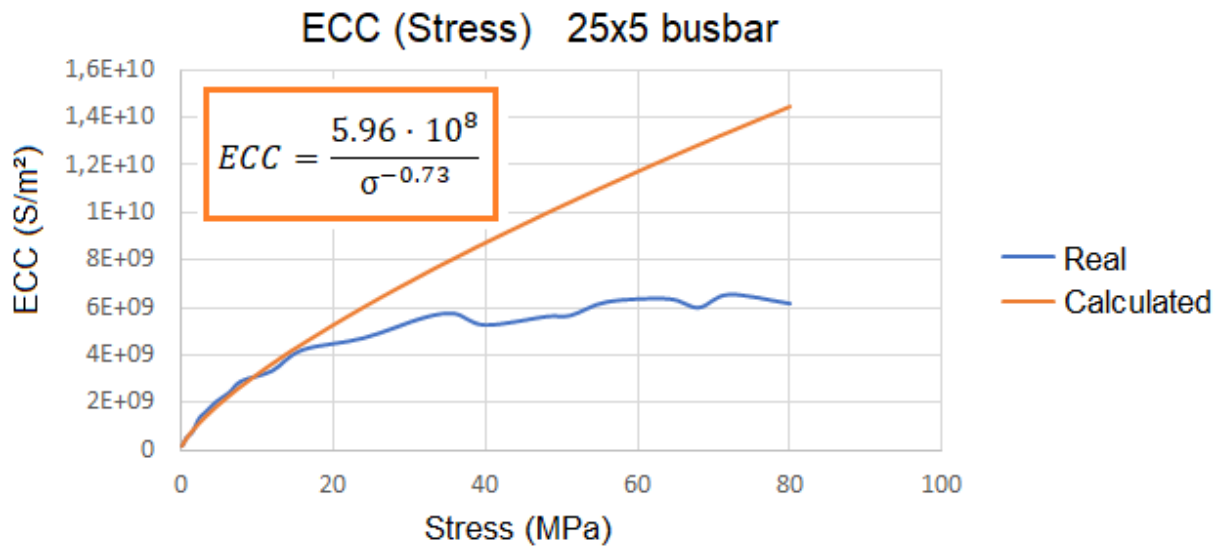
Table 3. 40x8 Rv comparison



Picture 27. Joint resistance comparison. 40x8 busbar



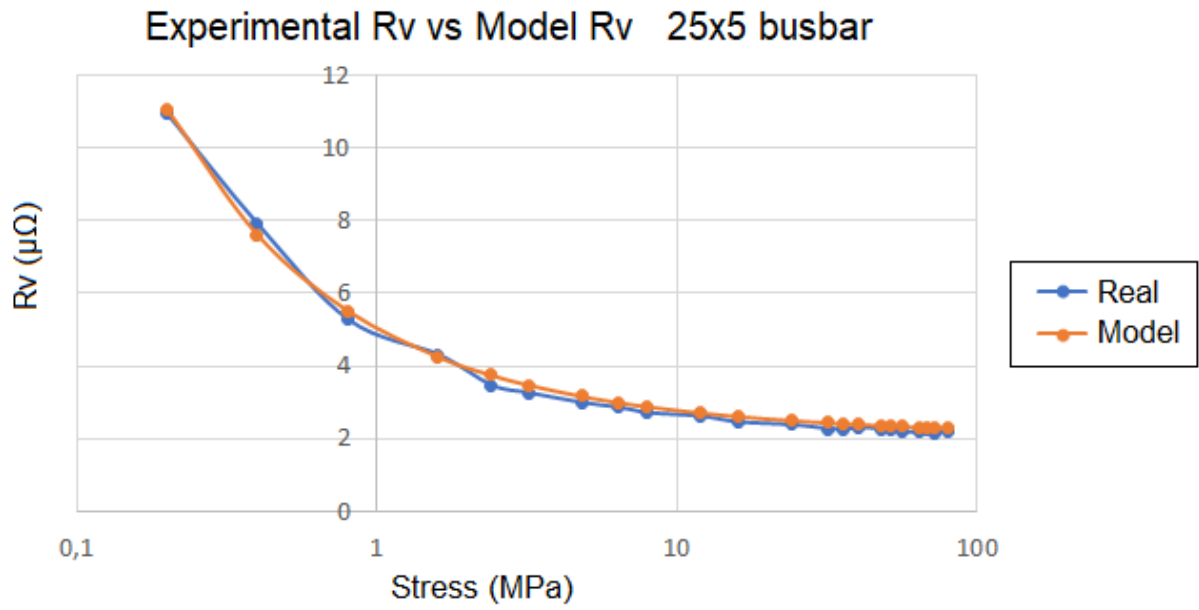
Picture 28. Real vs general model joint resistance, 40x8 busbar



Picture 29. ECC (Stress) fitted curve for 25x5 busbar

25x5 busbar		
Stress (MPa)	Rv (real) $\mu\Omega$	Rv (Model) $\mu\Omega$
0,2	10,93	11,03
0,4	7,90	7,59
0,8	5,27	5,51
1,6	4,31	4,25
2,4	3,47	3,75
3,2	3,26	3,47
4,8	2,99	3,17
6,4	2,86	2,99
8	2,71	2,88
12	2,61	2,71
16	2,45	2,61
24	2,38	2,50
32	2,27	2,44
36	2,25	2,41
40	2,31	2,39
48	2,26	2,36
51,2	2,26	2,35
56	2,19	2,33
64	2,18	2,31
68	2,22	2,30
72	2,16	2,30
80	2,20	2,28

Table 4. 25x5 Rv comparison



Picture 30. Rv comparison. 25x5 busbar